

FACILITY FORM 602

N66-22220
(ACCESSION NUMBER)

12
(PAGES)

TMX-56684
(NASA CR OR TMX OR AD NUMBER)

(THRU)

1
(CODE)

05
(CATEGORY)

HUMAN TRANSFER FUNCTIONS FOR MULTI-AXIS AND MULTI-LOOP PROBLEMS

By James J. Adams

NASA Langley Research Center
Langley Station, Hampton, Va.

Presented at the AIAA Fourth Manned Space Flight Meeting

St. Louis, Missouri
October 11-15, 1966

GPO PRICE \$ _____

CFSTI PRICE(S) \$ _____

Hard copy (HC) 1.00

Microfiche (MF) .50

TMX 56684

By James J. Adams

NASA Langley Research Center
Langley Station, Hampton, Va.~~Available to NASA only~~
~~Available to NASA only~~

Introduction

At Langley Research Center, pilot response in closed-loop control systems has been measured using an automatic, parameter-tracking, model-matching method. Response in single-axis, compensatory-tracking tasks with a variety of controlled elements was reported at a previous meeting.¹ These previously reported data restated, in a quantitative way, the fact that pilots prefer to control a vehicle which has some damping. The present paper will present data on multi-axis pilot response which illustrates an upper limit on response that is felt to be a limit on the pilot's information processing capacity. The application of these data to a multi-loop command maneuver will also be presented.

Method

The measurements that were made in the multi-axis tests were the transfer function of the pilot. These measurements were made by matching an analog model to the pilot by automatically adjusting three gains in the model. The model is constructed with analog computing equipment, and the analytical form for this model is

$$\frac{\text{Output}}{\text{Input}} = \frac{K_1 \tau \left(1 + \frac{K_2}{\tau} s \right)}{(\tau + s)^2}$$

and the gains K_1 , K_2 , and τ are adjusted to provide the best possible match to the pilot. An example of the ability of the parameter-tracking method to identify a known system is presented in figure 1. In this test the known system was of the same form as that selected for the adjustable model and was given gains of $K_1 = 7.5$, $K_2 = 7.5$, and $\tau = 7.5$. This system, or analog pilot, was placed in a control loop with dynamics of $\frac{K_3}{s(s+1)}$. The adjustable model was given initial values of $K_1 = 5$, $K_2 = 5$, $\tau = 10$. It can be seen from the figure that the adjustable model quickly matches the known model and arrives at the desired gain values.

It has been shown² that the transfer functions, or analog models, of human pilots determined by this parameter-tracking method can be substituted back in the control loop in place of the pilot and give a fairly good reproduction of the control exercised by the human. In the cases tried, the difference between the response obtained with the model and the human is that the model always controls better than the human.

The multi-axis data which will be presented were obtained using a fixed-base simulator. A three-axis artificial horizon, eight-ball instrument was used for the display, and a two-axis, sidearm controller and rudder pedals were used to exercise control. The vehicle dynamics being controlled were rate systems in which vehicle rate was a function of

controller displacement with a first-order lag of 1 second

$$\frac{K_3}{s(s+1)}$$

or acceleration systems, in which vehicle acceleration was a function of controller displacement, $\frac{K_3}{s^2}$, and were the same on each axis. The forcing

function was a random signal with a low cut-off frequency, 0.25 radian per second, and therefore the controlled errors that occurred on each axis were small, always less than 30° except for widely spaced instances. The response on each axis was therefore considered as three uncoupled systems, and was analyzed on this basis. The pilot's transfer functions were measured, and the closed-loop system characteristics were calculated.

Multi-Axis Tests

Four NASA test pilots were used as subjects in these tests. The subjects were tested in pitch, roll, and yaw separately, then in the combination of pitch and roll and finally in the combination of pitch, roll, and yaw. A sample time history of the roll response in a three-axis test is shown in figure 2. The figure illustrates the match that is achieved between the human and the model. The figure also illustrates the time variation in the measured model gains that is typically encountered in multi-axis tests. It can be seen that the gain K_1 is momentarily reduced from a nominal value at intervals during the run. These time variations are not present in single-axis test results.

In addition to the time variations in the measured gains, these are also changes in the nominal values of the gains which are a function of the number of axes being controlled. Sample results for one subject are presented in table I. The table presents the measured gains, the closed-loop system characteristics obtained using these measured gains, and the root-mean-square error and normalized error. The closed-loop characteristics were obtained by using the derived analytical expression for the pilot together with the given analytical expression for the vehicle and conventional block diagram algebra. The line labeled P_1 gives data for a pitch-only test; P_2 gives the pitch response in a pitch and roll test, etc., R and Y refer to roll and yaw. The data given for the single-axis tests are very similar to what has been reported previously. The new point that is illustrated by the data is that as additional axes for control are added to the pilot's task, the system frequency is reduced. For the pitch-only test the system frequency is 3.83 radians per second. The pitch response in a pitch and roll test shows a frequency of 3.26 radians per second. The overall average for all subjects for the ratio of two-axis system frequency to single-axis system frequency was 0.77, and for three

axes to single axis, the ratio was 0.66. The root-mean-square error follows an inverse relationship to this frequency change. It is felt that this reduction in frequency as the work load is increased represents the effect of an upper limit on the pilot's information processing capacity, and that perhaps a general rule relating information content of the task and system performance can be formulated.

Multi-Loop Problems

Another type of control situation that is encountered in control of vehicles is the multi-loop type of problem, as distinguished from a multi-axis problem. In a multi-loop situation there are two or more variables each of which is dependent on the other, as opposed to the multi-axis problem in which there are two or more variables which are independent. An example of the multi-loop problem is the translation control of a lunar landing vehicle, or a helicopter. In this type of system the vehicle is controlled in attitude to obtain the horizontal thrust required to bring about a desired change in horizontal displacement. To further show the distinction between a multi-axis and multi-loop problem the block diagrams of the two types of systems are shown in figure 3. For a multi-axis problem the system is considered to be made up of a number of control loops that are equal to the number of degrees of freedom with a separate pilot block in each loop. In a dual-loop problem, such as the lunar landing problem, the block diagram consists of an inner loop, containing a pilot block and a vehicle block, and around this inner loop is located an outer loop also containing a pilot block and a vehicle block. Again there are two pilot blocks, one for each variable in the problem, but now they are arranged in series. The outer-loop pilot block generates the command signal for the inner loop.

The transfer functions measured in the multi-axis tests have been applied to the multi-loop problem in an attempt to reproduce the time history of the human pilot to a step translation command in a simulated lunar landing control problem.

The time histories of the human-controlled response to a 1000-foot translation command and the response obtained using the analog models for the pilot are shown in figure 4.

The human-controlled response was obtained using a very simple simulator. The vehicle attitude was displayed using a small dial. The dial was mounted on the moving carriage of an X-Y plotter, and the motion of the plotter represented the translation of the vehicle. The subject used a side-to-side motion of a control stick to control vehicle attitude. Figure 4 shows that the subjects controlled vehicle attitude in a poorly damped manner, and the translation in a well-damped manner, and that the response obtained with the model reproduces these same characteristics.

The closed-loop system characteristic of these modes of motion are presented in table II. The pilot transfer functions used for the inner loop were taken from the data presented in table I. The two-axis roll response was used because the conditions under which this response was measured corresponded to the attitude control task in the multi-loop problem. The outer-loop characteristics, together with the pilot transfer function gains

used in obtaining them, are also presented. These characteristics for the outer loop alone show an overdamped response. The characteristics of the complete system combining both inner and outer loop are also presented. Comparing the complete system characteristics with the individual loop characteristics shows that there is interaction between the two modes of motion, with the damping of the attitude mode of motion being affected most.

The use of the pilot transfer functions presented in table II does reproduce the main features of the response obtained in a simulation of a multi-loop task. However, the response obtained with these constant coefficient, linear functions is better behaved than that achieved with a human subject. The measurements of human transfer functions in multi-axis problems show time variations in the coefficients, indicating what is felt to be a switching of attention on the part of the pilot from one variable to another, and even switching from the position signal to the rate signal on a given axis. This factor was not included in the models used in obtaining the time history of figure 4. Some exploratory tests have shown that by opening the inner loop for brief periods of time, representing a reduction in static gain to zero of the inner loop pilot, the randomness of the human response can be duplicated. It is felt that this switching of attention is another factor that should be related to the information content of the problem.

Damper Failure Problem

If the model representation of the human used in obtaining the time history of figure 4 really does represent the human, then the same model should also specify the instability that can occur in such a system when the damper in the inner loop fails. It is assumed that the pilot does not change his response for some short period of time following the damper failure. Examples of the human's response to such unsuspected damper failures are shown in figure 5. The figures show that one to two cycles of divergent attitude oscillation occur after the damper failure. Calculation of the system characteristics using the transfer functions of the pilot, both before and after the damper failure, are shown in table III. With the normal system the attitude mode of motion (the oscillatory characteristics with the frequency of 1.49 radians per second) has a positive damping ratio. When the damping is removed from the vehicle dynamics the attitude mode of motion goes unstable. Further, when the representative transfer function for the pilot is changed to that which was measured with an undamped vehicle the system again becomes stable, although with a lower damping ratio than existed with the damped vehicle.

Application to a Design Problem

Since the pilot model is able to correctly specify system characteristics over a variety of conditions, it is felt that it is a good representation. It was therefore decided to apply the model to a design problem. The problem concerns the design of the drive systems for a full-scale lunar landing simulator. The purpose of this simulator is to provide a $400 \times 165 \times 50$ foot volume in which a lunar landing type vehicle can maneuver under its own power. Five-sixth of the weight of the vehicle is supported by an overhead support

mechanism which is automatically controlled to remain directly above the vehicle. Certain design compromises were required in the translation drive system of this support mechanism by the presence of high-frequency structural vibrations. The two time histories presented in figure 6(a) of vehicle velocity response to thrust impulses are two points on the boundary of system performance specified by this necessary compromise. The restriction imposed by the structural vibration problem was to the damping that could be provided for the oscillatory mode of motion shown in figure 6(a). It was possible to achieve either the relatively low-frequency, well-damped response shown in the curves labeled low gain system, or the higher frequency poorly damped response shown in the curve labeled high gain system. It was felt that a better decision on the suitability of either of these two design points could be made if an input to the system similar to that expected from a manually controlled maneuver were used. Therefore the design analysis was extended to include the multi-loop representation developed in the previous section, and the response both with and without the simulator drive dynamics included was determined. The results are shown in figure 6(b). The vehicle-alone response shown in figure 6(b) is the calculated expected response of the system in the lunar environment, and is used as a standard for comparison for the calculated response of the simulator. The simulator responses were obtained using the same pilot and vehicle transfer functions as were used in obtaining the vehicle-alone response. The results show that the differences in the two drive systems being considered will have an effect on the

response of the system, and that to achieve a proper simulation of a lunar landing maneuver, the high gain drive mechanism should be used.

Conclusions

It has been demonstrated that constant coefficient transfer function can give a good representation of human pilot response in closed-loop control systems, even multi-loop command guidance systems. A correct specification of system characteristics over a wide variety of conditions was shown, including the unstable condition that follows an unexpected damper failure. It cannot be claimed that it is possible to make an absolute prediction of the response of any man-vehicle combination because the catalog of human transfer functions available at this time is limited. However the functions which have been presented can be used to achieve a quantitative understanding of the characteristics of manually controlled systems, can be used to make comparison studies, and thus can be used to resolve design problems.

References

1. Adams, James J.; and Bergeron, Hugh P.: Measured Variations in the Transfer Function of a Human Pilot. Presented at AIAA/AFSC Vehicle Design and Propulsion Meeting, Dayton, Ohio, November 4-6, 1963.
2. Adams, James J.; and Bergeron, Hugh P.: Measurements of Human Transfer Function with Various Model Forms. NASA TN D-2394, 1964.

TABLE I.- SUMMARY OF DATA FOR MULTI-AXES TESTS

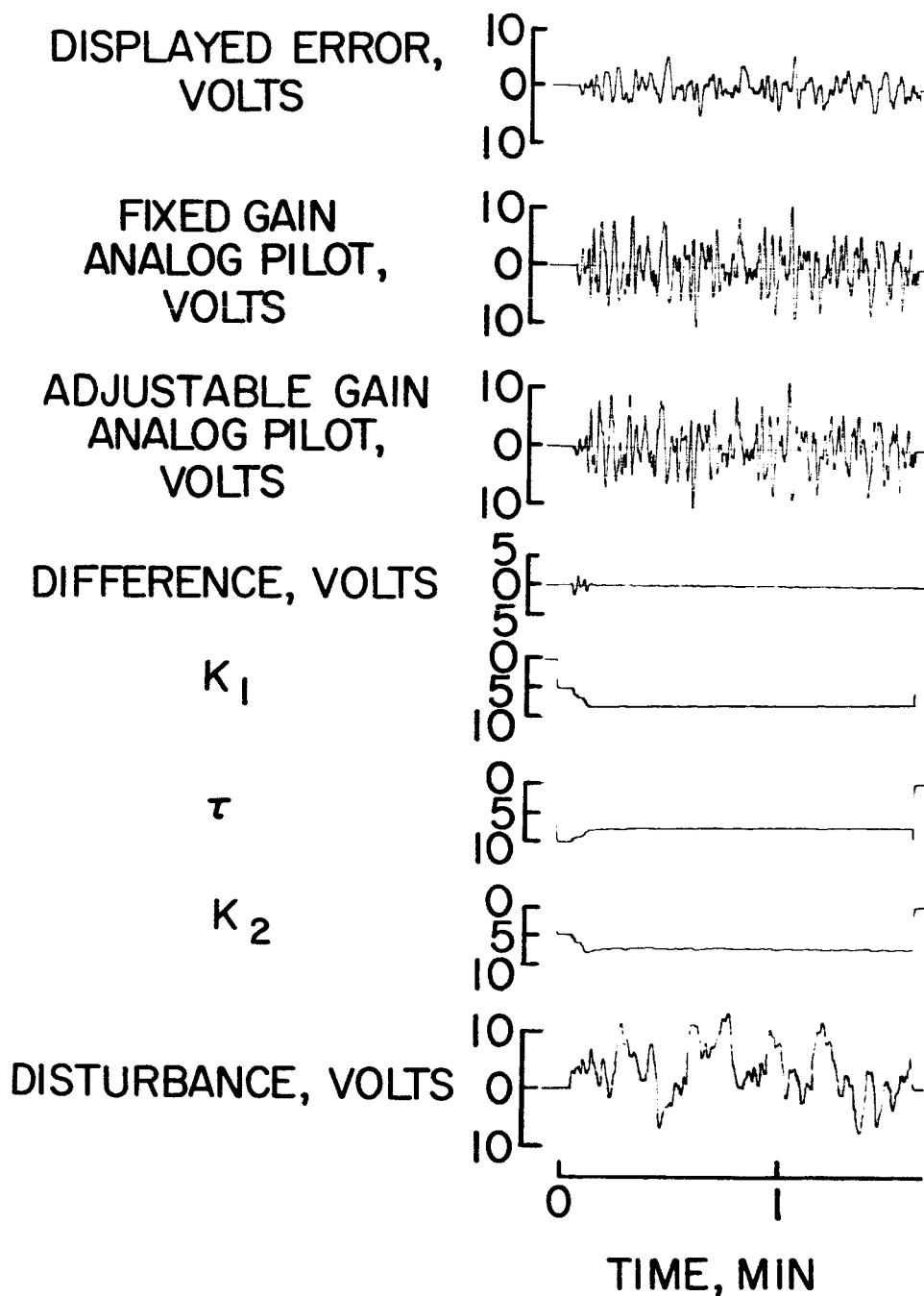
| Axis | Measured gains | | | Closed-loop characteristics | | | Root-mean-square error, volts | Normalized error | |
|--|----------------|-----|----------------|-----------------------------|------|--------------|-------------------------------|------------------|--|
| | | | | Oscillatory | | Real roots | | | |
| | K ₁ | τ | K ₂ | ω, rad/sec | ζ | | | | |
| Pilot J; Dynamics, $\frac{2}{s(s+1)}$; Disturbance break point frequency = 0.25 rad/sec | | | | | | | | | |
| P ₁ | 12 | 6.0 | 6.0 | 3.83 | 0.28 | -1.0, -9.83 | 0.99 | 0.108 | |
| P ₂ | 8.0 | 6.5 | 6.5 | 3.26 | .49 | -1.0, -9.76 | 1.22 | .133 | |
| P ₃ | 6.0 | 5.0 | 5.8 | 3.02 | .36 | -0.83, -7.98 | 1.41 | .154 | |
| R ₁ | 7.0 | 6.5 | 4.5 | 2.11 | .63 | -2.25, -9.06 | 1.62 | .177 | |
| R ₂ | 5.0 | 5.0 | 3.0 | 1.72 | .47 | -2.43, -6.96 | 2.39 | .262 | |
| R ₃ | 3.0 | 5.5 | 5.0 | 1.71 | .88 | -1.5, -7.49 | 2.80 | .306 | |
| Y ₁ | 6.0 | 5.0 | 3.0 | 1.93 | .42 | -2.26, -7.12 | 1.31 | .143 | |
| Y ₃ | 3.5 | 3.5 | 2.5 | 1.71 | .34 | -1.60, -5.24 | 2.27 | .249 | |
| Dynamics, $\frac{2}{s^2}$ | | | | | | | | | |
| P ₁ | 8.0 | 7.0 | 9.5 | 3.32 | 0.36 | -0.96, -10.6 | 1.16 | 0.127 | |
| P ₂ | 8.5 | 7.5 | 7.5 | 2.52 | .47 | -1.87, -10.8 | 1.89 | .206 | |
| P ₃ | 6.0 | 8.0 | 10 | 2.07 | .68 | -2.0, -11.1 | 2.5 | .274 | |
| R ₂ | 5.0 | 7.0 | 5.0 | 1.35 | .25 | -4.18, -9.15 | 3.41 | .383 | |
| R ₃ | 5.0 | 7.5 | 5.0 | 1.27 | .23 | -4.83, -9.6 | 3.42 | .384 | |
| Y ₃ | 5.5 | 7.0 | 7.5 | 1.24 | .35 | -5.60, -11.5 | 3.74 | .410 | |

TABLE II.- CLOSED-LOOP CHARACTERISTICS
FOR MULTI-LOOP EXAMPLE

| ω , rad/sec | ζ | Real roots |
|--|-------------|------------------------------|
| Inner loop alone Pilot gains: $K_1 = 5.0$, $K_2 = 3.0$, $\tau = 5.0$ Controlled element: $\frac{2}{s(s+1)}$ | | |
| 1.72 | 0.47 | -2.43, -6.56 |
| Outer loop alone Pilot gains: $K_1 = 0.09$, $K_2 = 42.0$, $\tau = 10.0$ Controlled element: $\frac{5.36}{s^2}$ | | |
| | | -0.176, -0.302, -7.60, -11.9 |
| Complete system, both loop configurations as given above | | |
| 1.40 10.2 | 0.33 .99 | -0.162, -0.410, -2.82, -6.40 |

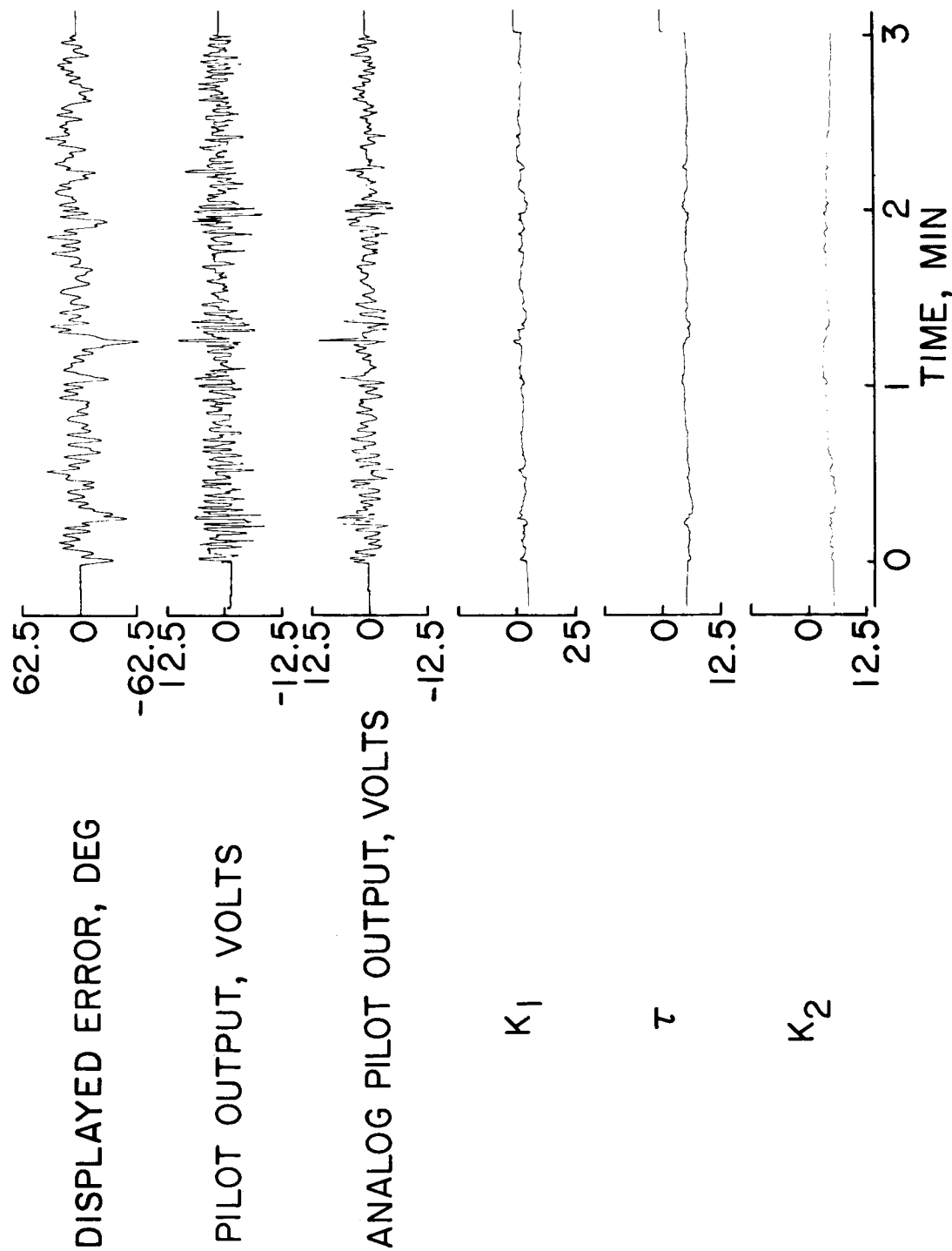
TABLE III.- CLOSED-LOOP CHARACTERISTICS
BEFORE AND AFTER A DAMPER FAILURE

| ω , rad/sec | ζ | Real roots |
|---|---------------|------------------------------|
| Normal system | | |
| 1.40 10.2 | 0.33 .99 | -0.162, -0.410, -2.82, -6.40 |
| After damper failure Inner-loop controlled element changed to $\frac{2}{s^2}$ | | |
| 1.54 10.2 | -0.077 .99 | -0.181, -0.269, -3.21, -6.31 |
| After pilot adaption to $\frac{2}{s^2}$ dynamics Pilot gains: $K_1 = 5.0$, $K_2 = 5.0$, $\tau = 7.0$ | | |
| 1.33 10.5 | 0.029 .99 | -0.185, -0.255, -4.77, -7.53 |



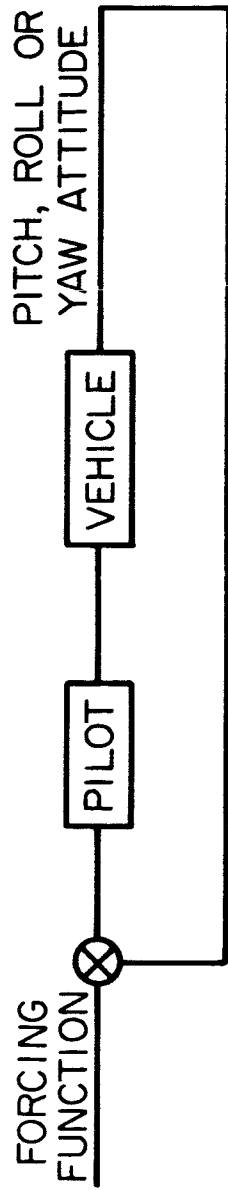
NASA

Figure 1.- Identification of a known system by parameter-tracking method.

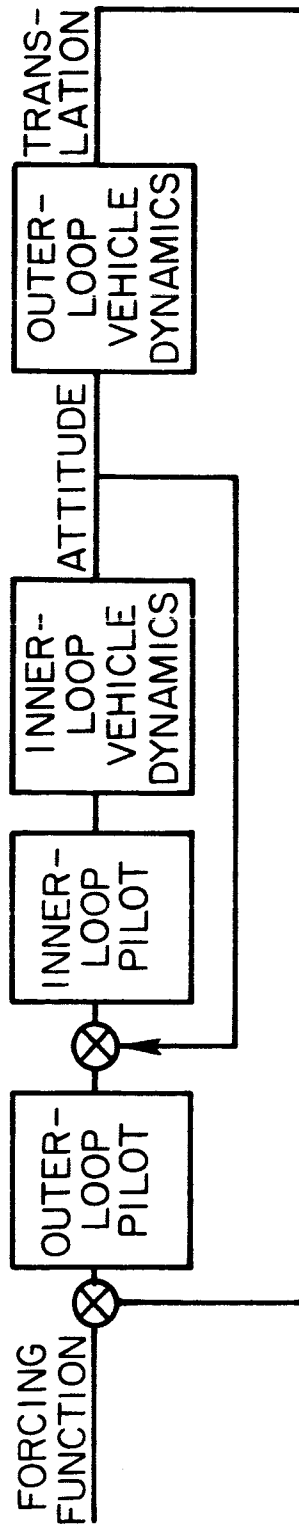


NASA

Figure 2.- Sample time history of model matching roll response in a three-axis test.

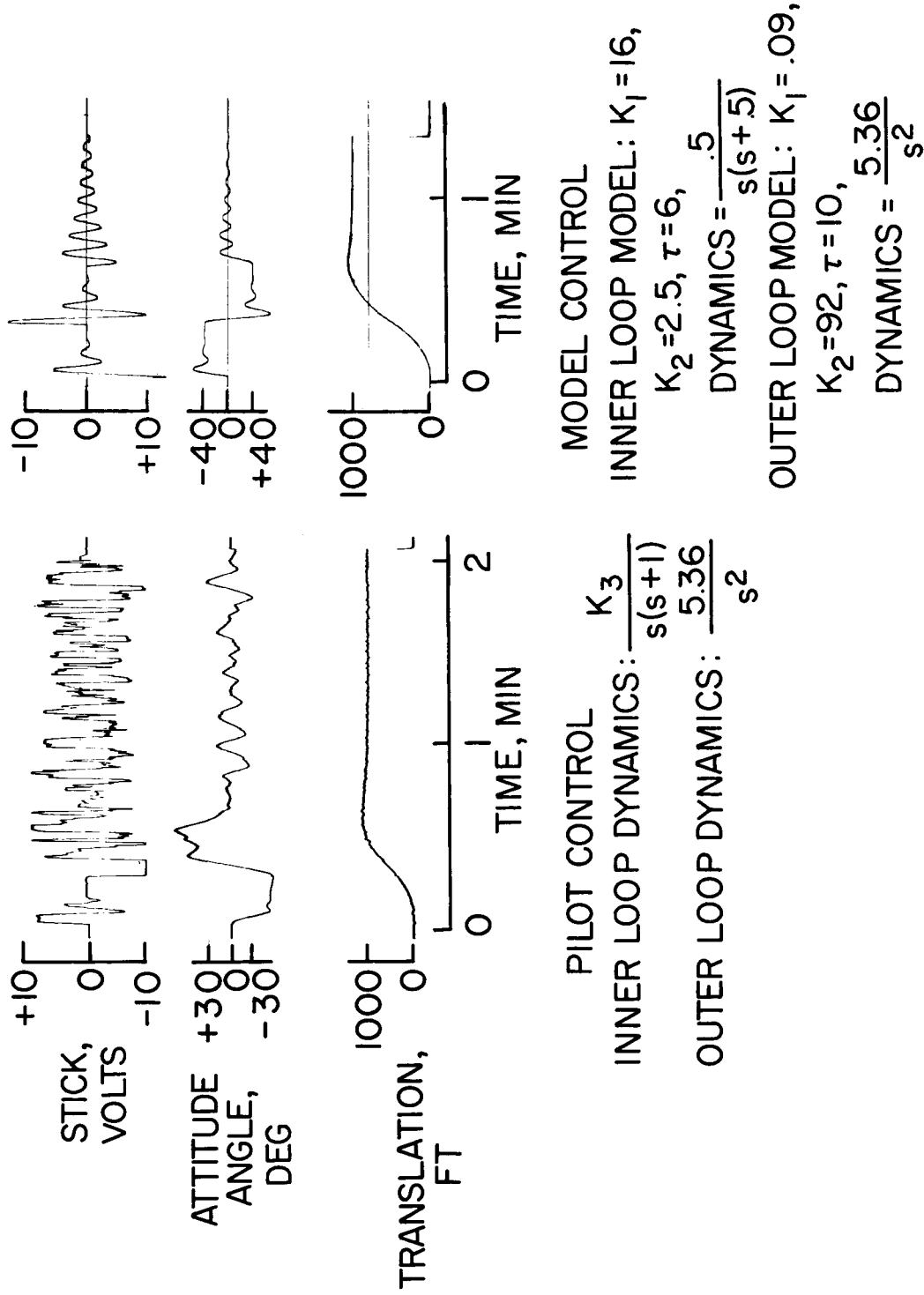


(a) Multi-axes diagram.



(b) Multi-loop diagram.

Figure 3.- Block diagrams for multi-axes and multi-loop systems.



NASA

Figure 4.- Comparison of response obtained in a multi-loop simulation with a human controller and with analog models for the pilot.

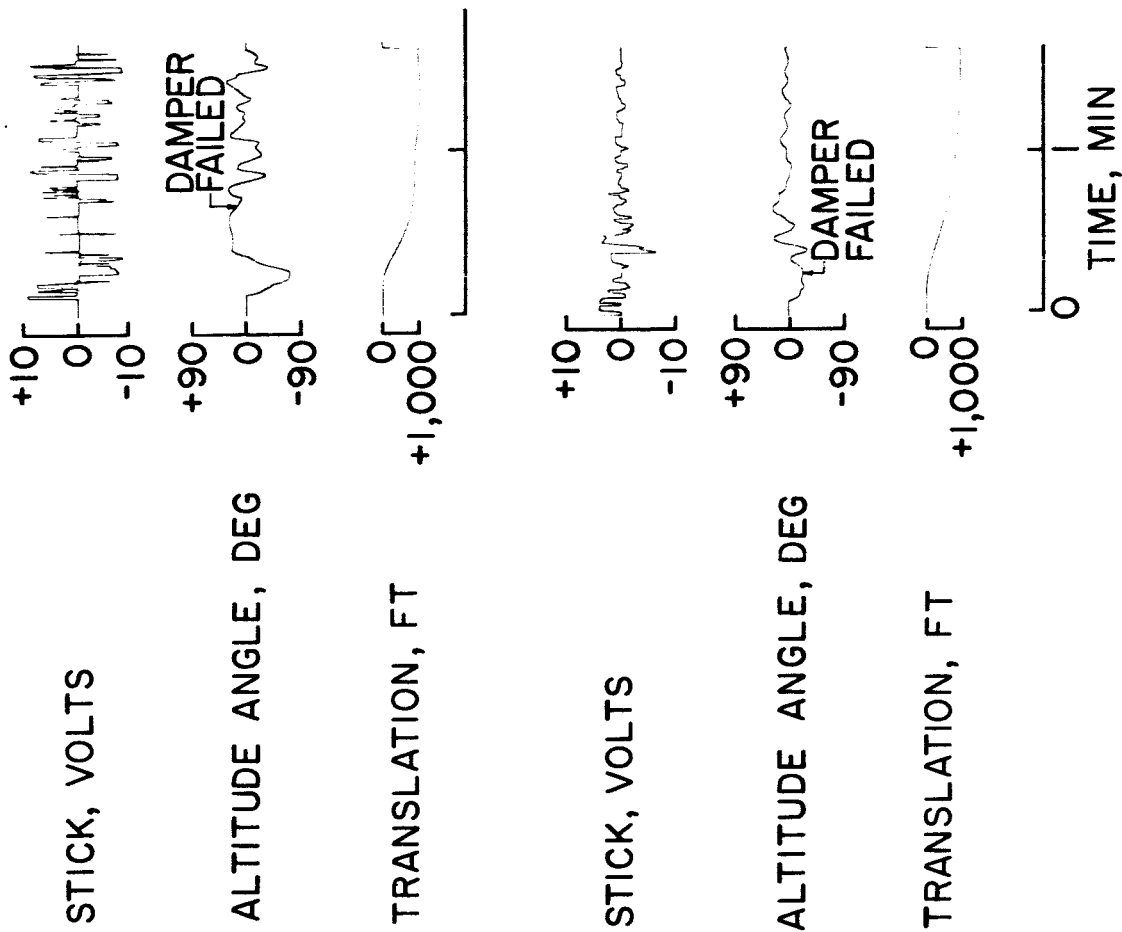
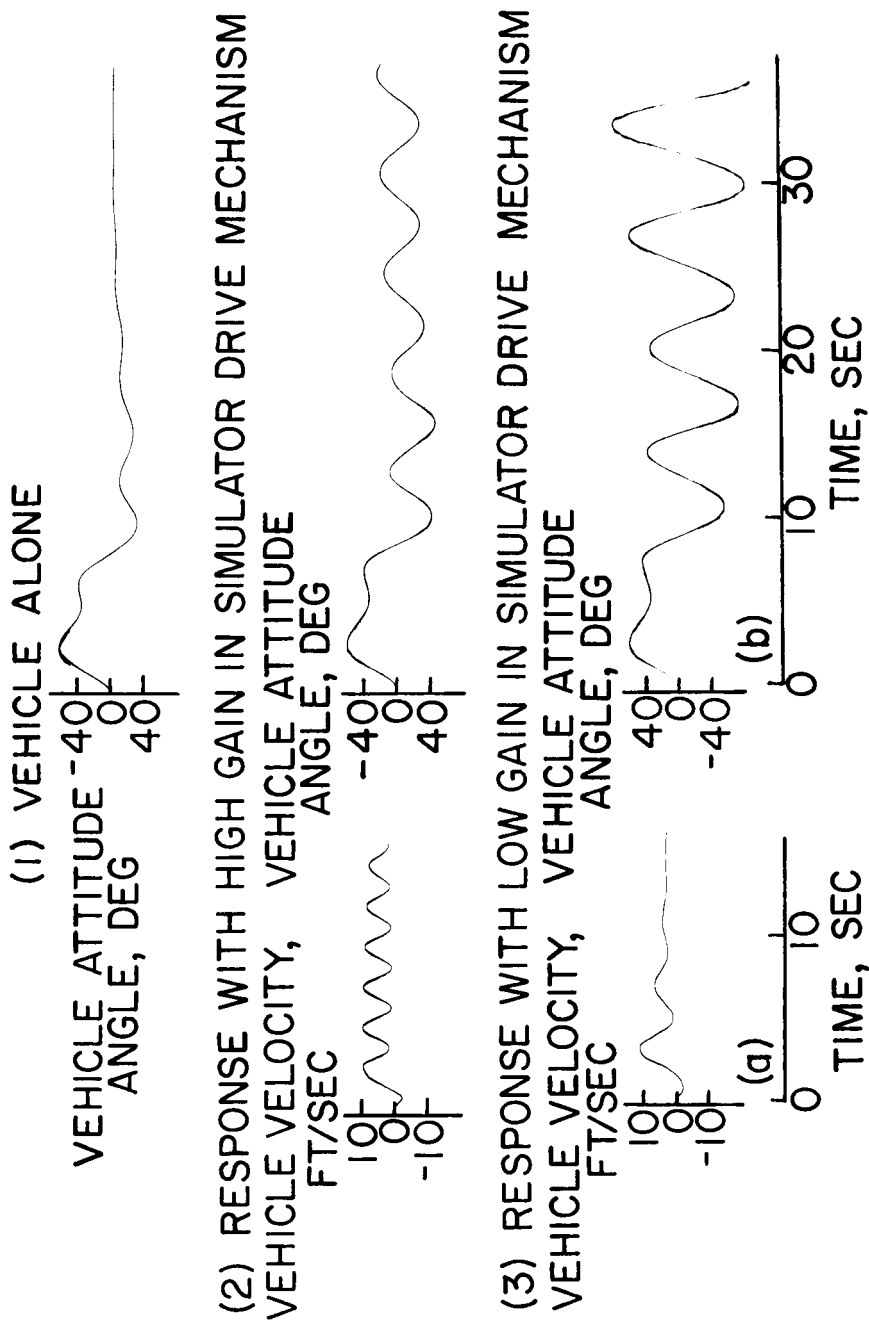


Figure 5.- Examples of manual control with unexpected damper failures.



NASA

Figure 6.- Response characteristics of simulator to step thrust inputs and to calculated pilot-controlled maneuver.